International Journal of Scientific & Engineering Research, Volume 4, Issue 10, October-2013
ISSN 2229-5518

Annulus with Spiral Slits Map and its Inverse of Bounded Multiply Connected Regions

[1,2]Ali W. Kareem Sangawi, [3]Ali H.M. Murid

Abstract:- This paper presents a boundary integral equation method for computing numerical conformal mapping of bounded multiply connected region onto an annulus with spiral slits region and its inverse. The method is an extension of the author's method for computing the Annulus with circular slits map of bounded multiply connected regions (see [Sangawi, A. W. K., Murid, A. H. M., Nasser, M. M. S.: Annulus with circular slit map of bounded multiply connected regions via integral equation method. Bull. Malays. Math. Sci. Soc. (2) **35**, no. 4, 945–959 (2012)]). Several numerical examples are given to prove the effectiveness of the proposed methods.

Index Terms— Numerical conformal mapping; Multiply connected regions; Generalized Neumann kernel.

1 Introduction

NEHARI and Wen [1–3] described the numbers of canonical regions of conformal mapping. Recently, reformulations of conformal mappings from bounded and unbounded multiply connected regions onto the five canonical slit regions as Riemann-Hilbert problems are discussed in Nasser [4–6]. An integral equation with the generalized Neumann kernel is then used to solve the RH problem as developed in [7]. A boundary integral equation method for mapping a bounded multiply connected region onto an annulus with circular slits region has been presented in [8]. And this result is extended by presenting a boundary integral equation method for numerical conformal mappings from a bounded multiply connected region onto an annulus with spiral slits region. The proposed method is based on linear boundary integral equation with adjoint generalized Neumann kernel which is constructed from a boundary relationship satisfied by an analytic function on a bounded multiply connected region.

Recently, in our several papers we have constructed new linear boundary integral equations for conformal mapping of bounded multiply region onto canonical slit regions [8–12], the first two papers regards to annulus and disk with slits are improves the work of Murid and Hu [13, 14].

The plan of the paper is as follows: Section 2 presents some auxiliary materials. Section 3 presents a method to calculate the piecewise real function h_j and υ_j. Section 4 presents the derivations of two integral equations related to S', $S(t)$, r_j and then f, respectively. In Section 5, we give some examples to illustrate our boundary integral equation method. Finally, Section 6 presents a short conclusion.

[1]*Department of Mathematics, School of Science, Faculty of Science and Science Education, Universiti of Sulaimani, 46001 Sulaimani, Kurdistan.*

[2]*Algebra and Computational Analysis Group (ACAG), Department of Mathematics, School of Science, Faculty of Science and Science Education, University of Sulaimani, 64001 UOS, Sulaimani, Kurdistan, Iraq, PH-009647701463002. E-mail: alisangawi2000@yahoo.com (Ali W. K. Sangawi)*

[3]*Department of Mathematical Sciences, Faculty of Science,Universiti Teknologi Malaysia and UTM Centre of Industrial and Applied Mathematics, 81310 UTM Johor Bahru, Johor, Malaysia, PH-0060127207253. E-mail: alihassan@utm.my (Ali H. M. Murid)*

2 Notations and Auxiliary Materials

Let Ω be a bounded multiply connected region of connectivity $M+1$. The boundary Γ consists of $M+1$ smooth Jordan curves Γ_j, $j=0,1,\ldots,M$ as shown in Figure 1.

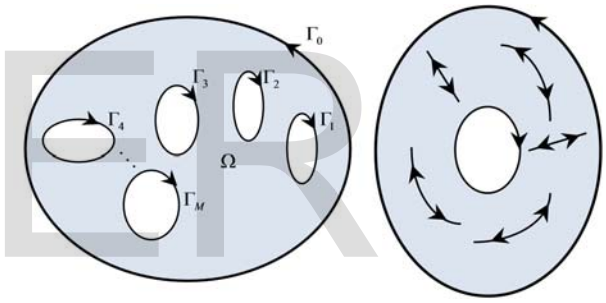

Figure 1 Mapping of the bounded multiply connected region Ω of connectivity M+1 onto an annulus with spiral slits

The curve Γ_j is parametrized by 2π-periodic twice continuously differentiable complex function $z_j(t)$ with non-vanishing first derivative

$$z_j'(t) = dz_j(t)/dt \neq 0, \quad t \in J_j = [0,2\pi], \quad j = 0,1,\ldots,M.$$

The total parameter domain J is the disjoint union of $M+1$ intervals $J_0,\ldots,J_M$. We define a parametrization $z(t)$ of the whole boundary Γ on J by

$$z(t) = z_j(t), \quad t \in J_j, \quad j = 0,1,\ldots,M. \tag{1}$$

Let H^* be the space of all real Hölder continuous 2π-periodic functions $\omega(t)$ of the parameter t on J_j for $j = 0,1,\ldots,M$, i.e.

$$\omega(t) = \omega_k(t), \quad t \in J_j, \quad j = 0,1,\ldots,M.$$

The unknown function $S(t)$ and $R(t)$ (a piecewise constant real function) will be given for $t \in J$ by

$$S(t) = S_j(t) \text{ and } R(t) = R_j(t), \quad t \in J_j, \quad j = 0, 1, \ldots, M.$$

Suppose that $c(z)$, $Q(z)$ and $H(z)$ are complex-valued functions defined on Γ such that $c(z) \neq 0$, $H(z) \neq 0$, $Q(z) \neq 0$ and $\overline{H(z)}/(T(z)Q(z))$ satisfies the Hölder condition on Γ . Then the interior relationship is defined as follows:

A complex-valued function $P(z)$ is said to satisfy the interior relationship if $P(z)$ is analytic in Ω and satisfies the non-homogeneous boundary relationship

$$P(z) = c(z)\frac{\overline{T(z)Q(z)}}{\overline{G(z)}}\overline{P(z)} + \overline{H(z)}, \qquad z \in \Gamma, \tag{2}$$

where $G(z)$ analytic in Ω, Hölder continuous on Γ, and $G(z) \neq 0$ on Γ. The boundary relationship (2) also has the following equivalent form:

$$G(z) = \overline{c(z)}T(z)Q(z)\frac{P(z)^2}{|P(z)|^2} + \frac{G(z)H(z)}{\overline{P(z)}}, \qquad z \in \Gamma. \tag{3}$$

The following theorem gives an integral equation for an analytic function satisfying the interior non-homogeneous boundary relationship (2) or (3), [10].

Theorem 2.1 *If the function $P(z)$ satisfies the interior non-homogeneous boundary relationship* (2) or (3), then

$$P(z) + \mathrm{PV}\int_\Gamma K(z,w)P(w)|dw| + c(z)\overline{T(z)Q(z)}$$

$$\times \left[\sum_{a_j \text{inside}\Gamma} \operatorname{Res}_{w=a_j} \frac{P(w)}{(w-z)G(w)}\right]^{\text{conj}} = -\overline{T(z)Q(z)}\,\overline{L_R^-(z)}, \; z \in \Gamma, \tag{4}$$

where

$$K(z,w) = \frac{1}{2\pi \mathrm{i}}\left[\frac{c(z)\overline{T(z)Q(z)}}{c(w)(\overline{w}-\overline{z})\overline{Q(w)}} - \frac{T(w)}{w-z}\right], \tag{5}$$

$$L_R^-(z) = \frac{-1}{2}\frac{H(z)}{Q(z)T(z)} + \mathrm{PV}\frac{1}{2\pi \mathrm{i}}\int_\Gamma \frac{\overline{c(z)}H(w)}{\overline{c(w)}(w-z)Q(w)T(w)}dw. \tag{6}$$

The symbole "conj" in the superscript denotes complex conjugate, while the minus sign in the superscript denotes limit from the exterior. The sum in (4) is over all those zeros $a_1, a_2, \ldots, a_M$ of G that lie inside Ω . If G has no zeros in Ω , then the term containing the residue in (4) will not appear.

3 Compute the piecewise real function h_j and υ_j

Let $\hat{A}(t)$ be a complex continuously differentiable 2π-periodic function for all $t \in J$. The generalized Neumann kernel formed with $\hat{A}$ is defined by

$$\hat{N}(t,s) = \frac{1}{\pi}\mathrm{Im}\left(\frac{\hat{A}(t)}{\hat{A}(s)}\frac{z'(s)}{z(s)-z(t)}\right),$$

$$\hat{N}(t,t) = \frac{1}{\pi}\left(\frac{1}{2}\mathrm{Im}\frac{z''(t)}{z'(t)} - \mathrm{Im}\frac{\hat{A}'(t)}{\hat{A}(t)}\right).$$

Define also the kernel $\hat{M}$ by

$$\hat{M}(t,s) = \frac{1}{\pi}\mathrm{Re}\left(\frac{\hat{A}(t)}{\hat{A}(s)}\frac{z'(s)}{z(s)-z(t)}\right),$$

which has a cotangent singularity type (see [7] for more detail). The adjoint function to the function $\hat{A}$ is given by

$$\tilde{A}(t) = \frac{z'(t)}{\hat{A}(t)}.$$

The generalized Neumann kernel $\tilde{N}(s,t)$ formed with $\tilde{A}$ is given by

$$\tilde{N}(t,s) = \frac{1}{\pi}\mathrm{Im}\left(\frac{\tilde{A}(t)}{\tilde{A}(s)}\frac{z'(s)}{z(s)-z(t)}\right).$$

Then

$$\tilde{N}(s,t) = -N^*(s,t),$$

where $N^*(s,t) = \hat{N}(t,s)$ is the adjoint kernel of the generalized Neumann kernel $\hat{N}(s,t)$ (see [7] for more detail). We define the Fredholm integral operator $\mathbf{N}^*$ by

$$\mathbf{N}^*\psi(t) = \int_J N^*(t,s)\psi(s)ds, \qquad t \in J.$$

It is known that $\lambda = 1$ is an eigenvalue of the kernel $\hat{N}$ with multiplicity 1 and $\lambda = -1$ is an eigenvalue of the kernel $\hat{N}$ with multiplicity $M+1$ [7]. The eigenfunctions of $\hat{N}$ corresponding to the eigenvalue $\lambda = -1$ are $\left\{\chi^{[0]}, \chi^{[1]}, \ldots, \chi^{[M]}\right\}$, where

$$\chi^{[j]}(\xi) = \begin{cases} 1, & \xi \in \Gamma_j, \\ 0, & \text{otherwise}, \end{cases} \qquad j = 0, 1, \ldots, M.$$

Then, we define the space $\hat{S}$ by

$$\hat{S} = \mathrm{span}\{\chi^{[0]}, \chi^{[1]}, \ldots, \chi^{[M]}\}. \tag{7}$$

We also define an integral operator $\mathbf{J}$ by (see [9])

$$\mathbf{J}\upsilon = \int_J \frac{1}{2\pi}\sum_{j=1}^{M}\chi^{[j]}(s)\chi^{[j]}(t)\upsilon(s)ds, \tag{8}$$

$$\hat{\mathbf{J}}\upsilon = \int_J \frac{1}{2\pi}\sum_{j=0}^{M}\chi^{[j]}(s)\chi^{[j]}(t)\upsilon(s)ds, \tag{9}$$

The following theorem gives us a method for calculating the piecewise real function,h and υ in canonical slit representation, hence r and $\hat{\upsilon}$, respectively. This theorem can be proved by using the approach as in Theorem 5 in [15].

Theorem 3.1 *The function $\gamma, \mu \in H^*$ and $h, \upsilon \in \hat{S}$ such that*

$$\hat{A}\hat{g} = \gamma + h + \mathrm{i}(\mu + \upsilon) \tag{10}$$

are boundary values of an analytic function $\hat{g}(z)$ in Ω. Then the function $h = (h_0, h_1, \ldots, h_m)$ and $\upsilon = (\upsilon_0, \upsilon_1, \ldots, \upsilon_m)$ are given by

$$h_j = (\gamma, \phi^{[j]}) = \frac{1}{2\pi}\int_\Gamma \gamma(t)\phi^{[j]}(t)dt, \tag{11}$$

$$\upsilon_j = (\mu, \phi^{[j]}) = \frac{1}{2\pi}\int_\Gamma \mu(t)\phi^{[j]}(t)dt, \tag{12}$$

where $\phi^{[j]}$ is solution of the following integral equation

$$(\mathbf{I} + \mathbf{N}^* + \hat{\mathbf{J}})\phi^{[j]} = -\chi^{[j]}, \qquad j = 0, 1, \ldots, m. \tag{13}$$

4 An Annulus with Spiral Slits Region

This canonical region consist of an annulus centered at origin a together with $M-1$ to the logarithmic spirals. Let $f(z)$ be the mapping function that maps a bounded multiply connected region onto the canonical region. We assume that $f(z)$ maps the curve Γ_0 onto a unit circle $|f(z)| = 1$, the curve Γ_1 onto the circle $|f(z)| = R_1$ and the curves $\Gamma_j, j = 2, 3, \ldots, M$ onto logarithmic spiral slit

$$\mathrm{Im}\left(e^{-\theta_j}\log f(z_j(t))\right) = R_j, \quad j = 2, 3, \ldots, M, \tag{14}$$

where $R_1, R_2, \ldots, R_M$ are undetermined real constants, and $\theta_j, j = 2, 3, \ldots, M$ is called as oblique angle of (14), represents the angle of intersection between the logarithmic spiral and ray emanating from origin, θ_j are given real constant. We choose $\theta_0 = \theta_1 = \pi/2$, then the boundary values of the mapping function $f(z)$ satisfies

$$\overline{B}\log f(z(t)) = r(t) + \mathrm{i}S(t), \tag{15}$$

where,

$$\overline{B} = e^{\mathrm{i}(\pi/2 - \theta_j)} \text{ and } r_j = \begin{cases} \ln R_0 = 0, & j = 0, \\ \ln R_1, & j = 1, \\ -R_j, & j = 2, 3, \ldots, M. \end{cases} \tag{16}$$

The mapping function $f(z)$ can be uniquely determined by assuming $f(0) > 0$, then the mapping function can be expressed as [6]

$$f(z) = c\left(1 - \frac{z}{z_1}\right)e^{z\hat{h}(z)}, \tag{17}$$

where $h(z)$ is an analytic function and $c = f(0)$ is an undetermined real constant, z_1 is a prescribed point inside Γ_M.

Let $F(z) = e^{\overline{B}\log(f(z))} = e^{r + \mathrm{i}S(t)}$ and then

$$F'(z_j(t)) = \mathrm{i}S_j'(t)F(z_j(t)), \quad j = 0, 1, ..., M. \tag{18}$$

Note that from (18) and using the fact that $T(z) = \dfrac{z'(t)}{|z'(t)|}$ can be shown that

$$F(z_j(t)) = \frac{|F(z_j(t))|}{\mathrm{i}}\frac{|S_j'(t)|}{S_j'(t)}T(z_j(t))\frac{F'(z_j(t))}{|F'(z_j(t))|}, \quad j = 0, 1, \ldots, M. \tag{19}$$

Note that $F(z)$ can be written in the following form

$$F(z) = e^{\overline{B}\log(z_1 - z)}e^{\overline{B}\hat{g}(z)}, \tag{20}$$

where $\hat{g}(z) = z\hat{h}(z) + \log(c) - \log(z_1)$, and then

$$D(z) = \frac{F'(z)}{F(z)} = \left[\overline{B}\hat{g}'(z) - \frac{\overline{B}}{z_1 - z}\right], \quad \text{is analytic in } \Omega \tag{21}$$

Note that the value of S_j' may be positive or negative since each slit $f(\Gamma_p)$ is traversed twice. Thus $\dfrac{|S_p'|}{S_p'} = \pm 1$. Hence the boundary relationship (19) can be written as

$$F(z_j(t)) = \pm\frac{|F(z_j(t))|}{\mathrm{i}\overline{T(z_j(t))}}\frac{F'(z_j(t))}{|F'(z_j(t))|}, \; j = 0, 1, \ldots, M. \tag{22}$$

To eliminate the $\pm$ sign, we square both sides of the boundary relationship (22), Yields

$$F(z)^2 = -|F(z)|^2T(z)^2\frac{F'(z)^2}{|F'(z)|^2}, \quad z \in \Gamma. \tag{23}$$

Combining (21) and (23), we obtain

$$D(z) = -\overline{T}(z)^2\overline{D}(z), \quad z \in \Gamma \tag{24}$$

By using the definition of $F(z)$, (23) becomes

$$F(z)^2 = -e^{2r_j}T(z)^2\frac{F'(z)^2}{|F'(z)|^2}, \quad z \in \Gamma. \tag{25}$$

By taking logarithmic on both sides of (20), we obtain

$$\log(F(z(t)) = \overline{B}\ln c + \overline{B}\log\left(\frac{z_1 - z(t)}{z_1}\right) + \overline{B}z(t)\hat{h}(z(t)). \tag{26}$$

And from the definition of $F(z)$, we obtain

$$\log(F(z_j(t)) = r_j + \mathrm{i}S_j(t), \tag{27}$$

where $r_0 = 0,\ r_1 = \ln R_1,\ r_k = -R_k,\ k = 2,\ 3,\ \ldots,\ M$, then

$$\begin{aligned}\overline{B}\hat{k}(z(t)) &= r_j + \mathrm{i}S_j(t) - \mathrm{Re}\left(\overline{B}\ln c\right) - \mathrm{i}\,\mathrm{Im}\left(\overline{B}\ln c\right) \\ &\quad -\overline{B}\log\left(\frac{z_1 - z(t)}{z_1}\right) \\ &= r_j + \mathrm{i}(\rho(t) + \hat{\upsilon}(t)) - \mathrm{Re}\left(\overline{B}\ln c\right) - \mathrm{i}\,\mathrm{Im}\left(\overline{B}\ln c\right) \\ &\quad -\overline{B}\log\left(\frac{z_1 - z(t)}{z_1}\right) \\ &= \gamma(t) + h(t) + \mathrm{i}(\rho(t) + \mu(t) + \upsilon(t)),\end{aligned} \tag{28}$$

where $\gamma(t) = \mathrm{Re}\left(-\overline{B}\log\left(\frac{z_1 - z(t)}{z_1}\right)\right)$, $\mu(t) = \mathrm{Im}\left(-\overline{B}\log\left(\frac{z_1 - z(t)}{z_1}\right)\right)$, $h(t) = r_j - \mathrm{Re}\left(\overline{B}\log(c)\right)$ and $\upsilon(t) = \hat{\upsilon}(t) - \mathrm{Im}\left(\overline{B}\log(c)\right)$.
By obtaining $h_j,\ j = 0, 1, \ldots, M$, from (11) we obtain

$$c = e^{\frac{-h_0}{\sin\theta_0}}, \tag{29a}$$

and

$$r_j = h_j + \mathrm{Re}\left(\overline{B}\log(c)\right), \quad j = 1, 2, \ldots, M. \tag{29b}$$

Note that from (17) can be shown that

$$\left|\frac{f'(z)}{f(z)}\right| l(z) = \frac{f'(z)}{f(z)}\,|l(z)|, \tag{30}$$

where $l(z) = z\hat{h}'(z) + \hat{h}(z) - \dfrac{1}{z_1 - z}$, is analytic in Ω. Square both sides of the above boundary relationship using (15) and the fact that $T(z) = \dfrac{z'}{|z'|}$, Yields

$$l(z) = -B\overline{T(z)^2\overline{B}}\,\overline{l(z)}, \quad z \in \Gamma, \tag{31}$$

Comparison (31) and (2) leads to a choice of $P(z) = l(z)$, $Q(z) = T(z)\overline{B}$, $C(z) = -B$, $G(z) = 1$, and $H(z) = 0$, Theorem 2.1, yields

$$\begin{aligned}l(z) + \mathrm{PV}\frac{1}{2\pi\mathrm{i}}\int_\Gamma \left[\frac{B(z)\overline{T(z)^2}B(z)}{B(w)(\overline{w} - \overline{z})\overline{T(z)}B(w)} - \frac{T(w)}{w - z}\right] \\ \times l(w)|dw| = 0,\end{aligned} \tag{32}$$

After some algebraic manipulation and using the fact that $B\overline{B} = 1$, Obtain the following Integral equation

$$\begin{aligned}\overline{B(z)}l(z)T(z) + \mathrm{PV}\frac{1}{2\pi\mathrm{i}}\int_\Gamma \left[\frac{\overline{B(z)}T(z)}{\overline{B(w)}(z - w)} - \frac{\overline{\overline{B(z)}T(z)}}{\overline{\overline{B(w)}}(\overline{z} - \overline{w})}\right] \\ \times\overline{B(w)}l(w)T(w)|dw| = 0\end{aligned} \tag{33}$$

In the above integral equation let $z = z(t)$ and $w = z(s)$. Then by multiplying both sides of (33) by $|z'(t)|$ and using the fact that

$$l(z_j(t))z_j'(t)\overline{B(z_j(t))} = \mathrm{i}S_j'(t), \quad j = 0, 1, \ldots, M,$$

the above integral equation can also be written as

$$S_j'(t) + \int_J \hat{N}(s,t)S_j'(s)ds = 0, \quad j = 0, 1, \ldots, M.$$

Since $\hat{N}^*(s,t) = \hat{N}(t,s)$, the integral equation can be written as an integral equation in operator form

$$(\mathbf{I} + \hat{\mathbf{N}}^*)S_j' = 0, \quad j = 0, 1, \ldots, M, \tag{34}$$

where $\lambda = -1$ is an eigenvalue of $\hat{N}^*$ with multiplicity M by Theorem 12 in [7]. By using the fundamental theorem [16, p.164] and using the fact that $T(w)\,|dw| = dw$, gives

$$\int_{-\Gamma_j} \frac{1}{2\pi}T(w)\frac{F'(w)}{F(w)}\,|dw| = \begin{cases} \mathrm{i}, & j = M, \\ 0, & j = 1, 2, \ldots, M-1, \end{cases} \tag{35}$$

which implies that

$$\mathbf{J}S_j' = (0, \ldots, 0, -1), \quad j = 1, 2, \ldots, M. \tag{36}$$

By adding (36) to (34), we obtain the equation

$$(\mathbf{I} + \hat{\mathbf{N}}^* + \mathbf{J})S' = \hat{\phi}(t), \tag{37a}$$

where

$$\hat{\phi}(t) = (0, \ldots, 0, -1). \tag{37b}$$

In view of the following theorem, the integral equation (37) is uniquely solvable (see [9]).

Theorem 4.1

$$\mathrm{Null}(\mathbf{I} + \hat{\mathbf{N}}^* + \mathbf{J}) = \{0\}. \tag{38}$$

Notice that the function $S_j(t)$ for $j = 0, 1, \ldots, M$, can be calculated from $S_j'(t)$ by

$$S_j(t) = \int S_j'(t)dt + \upsilon_j =: \rho_j(t) + \upsilon_j, \quad t \in J_j, \tag{39}$$

where υ_j is undetermined real constant and the real function $\rho_j(t)$ is defined by

$$\rho_j(t) = \int S_j'(t)dt, \quad t \in J_j. \tag{40}$$

The unknown function $S_j(t)$ is not necessary a 2π-periodic. However, it's derivative $S_j'(t)$ is 2π-periodic. Thus, the function $S_j'(t)$ can be represented by a Fourier series

$$S_j'(t) = a_0^{[j]} + \sum_{k=1}^{\infty} a_k^{[j]}\cos kt + \sum_{k=1}^{\infty} b_k^{[j]}\sin kt, \quad t \in J_j. \tag{41}$$

Hence the function $\rho_j(t)$ can be calculated by Fourier series representation as

$$\rho_j(t) = a_0^{[j]}t + \sum_{k=1}^{\infty}\frac{a_k^{[j]}}{k}\sin kt - \sum_{k=1}^{\infty}\frac{b_k^{[j]}}{k}\cos kt, \quad t \in J_j. \tag{42}$$

By solving the integral equation (37) we get $S_j'(t)$. And solving the integral equation (13) we get $\phi^{[j]}$, $j=0,1,\ldots,M$, which gives h_j through (11) which in turn gives c and r_j through (29). By solving (41) and (42) we get the value of ρ through (12) we get the value of υ_j which in turn gives $\hat{\upsilon}_j$ The approximate boundary value of $f(z)$ is given by

$$f(z_j(t)) = e^{B\left(r_j+\mathrm{i}\left(\rho_j(t)+\hat{\upsilon}_j(t)\right)\right)}, \quad j=0,1,\ldots,M. \tag{43}$$

The approximate interior value of the function $f(z)$ is calculated by the Cauchy integral formula

$$f(z) = \frac{\int_\Gamma \frac{f(w)}{w-z}dw}{\int_\Gamma \frac{1}{w-z}dw}, \qquad z\in\Omega. \tag{44}$$

The integrals in the numerators has the advantage that the denomenator in this formula compensates for the error in the numerator (see [17]). The integrals in (44) are approximated by the trapezoidal rule.

For computing the inverse maps, noted that the mapping function $f^{-1}(w)=z$ is analytic in the region annulus with spiral slit with a simple pole at $w=c$. Let an analytic function $\phi(w)$ be defined as

$$\phi(w) = (w-c)z = (w-c)f^{-1}(w)$$

Then by using Cauchy integral formula, we obtain $z\in\Omega$ by

$$z = \frac{1}{(w-c)2\pi\mathrm{i}}\int_J \frac{(f(z(t))-c)z(t)}{f(z(t))-w}BiS'(t)f(z(t))dt$$

5 Numerical Examples

Since the function $z_p(t)$ is 2π-periodic, a reliable procedure for solving the integral equations (37) and (13) numerically is by using the Nyström's method with the trapezoidal rule [18]. The trapezoidal rule is the most accurate method for integrating periodic functions numerically [19, pp.134-142]. The algebraic linear systems is uniquely solvable for sufficiently large number of collocation points on each boundary component, since the integral equations (13) and (37) are uniquely solvable [20]. The computational details are similar to [4,5,13,14].

For numerical experiments, we have used some test regions with smooth and non-smooth boundaries of connectivity three, four, seven and ten based on the examples given in [4,6]. All the computations were done using MATLAB R2011a. The number of points used in the discretization of each boundary component Γ_j is n. The test regions and their corresponding images are shown in Figures 2-7.

Example 5.1 *Consider the region bounded by three ellipses given in Nasser [4]:*

$$\begin{aligned}
\Gamma_0 : \{z(t) &= 10\cos t + 6\mathrm{i}\sin t\},\\
\Gamma_1 : \{z(t) &= -4-2\mathrm{i}+3\cos t - 2\mathrm{i}\sin t\},\\
\Gamma_2 : \{z(t) &= 4+2\cos t - 3\mathrm{i}\sin t\},\ 0\le t\le 2\pi,\\
z_1 &= 4,\ \theta = \left(\frac{\pi}{2},\frac{3\pi}{4},\frac{\pi}{2}\right).
\end{aligned}$$

Figure 2 shows the region and its image, and Figure 3 shows the annulus with spiral slit and its inverse image based on our method. See Table 1 for comparison between our computed values of c and R_i, $i=1,2$ with those computed values of Nasser [6]

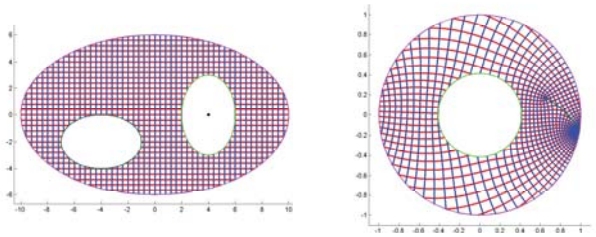

Figure 2 Mapping a region of connectivity three onto an annulus with spiral slit.

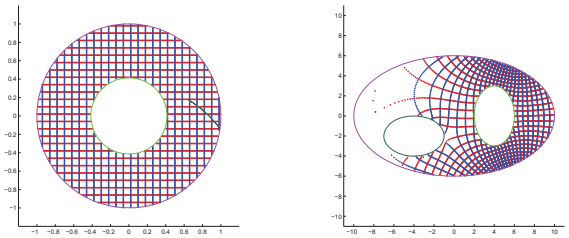

Figure 3 Inverse image of the annulus with spiral slit.

Table 1 Radii comparison for Example 5.1 with [6]

n	32	64	128
$\|c-cN\|_\infty$	7.6(−07)	7.0(−12)	8.8(−16)
$\|R_1-RN_1\|_\infty$	4.3(−06)	4.4(−10)	6.6(−16)
$\|R_2-RN_2\|_\infty$	1.5(−06)	3.8(−10)	2.2(−16)

Example 5.2 *Consider the region of connectivity seven and ten, [6],*

$$z_j(t) = \xi_j + e^{\mathrm{i}\sigma_j}(a_j\cos t + \mathrm{i}b_j\sin t), \quad j=0,1,\ldots,9, \tag{45}$$

The values of the complex constants ξ_j and the real constants a_j, b_j and σ_j are as in Table 2 and the values of $z_1 = -0.8330 - \mathrm{i}2.1650$ and $\theta = \left(\frac{\pi}{2},\frac{\pi}{2},\frac{\pi}{4},0,\frac{\pi}{4},0,\frac{\pi}{2},\frac{2\pi}{3},\frac{5\pi}{3},\frac{3\pi}{2}\right)$. Mapping function from the original region onto the annulus with spiral slits region and the inverse mapping functions from the annulus with spiral slits region onto the original region. The numerical results are presented in Figures 4–7. See Tables 3 and 4 for comparison between our computed values of c and R_i, $i=1,2,\ldots,6$ with those computed values of Nasser [6] and computed values of c and R_i, $i=1,2,\ldots,9$.

Table 2 The values of constants a_j, b_j, ξ_j and σ_j in (5.2).

j	a_j	b_j	ξ_j	σ_j
0	4.0000	3.0000	$-0.5000-\mathrm{i}0.5000$	1.0000
1	0.2976	-0.6132	$-0.8330-\mathrm{i}2.1650$	5.7197
2	0.5061	-0.6053	$-1.7059+\mathrm{i}0.3423$	0.5778
3	0.6051	-0.7078	$0.3577-\mathrm{i}0.9846$	4.1087
4	0.7928	-0.3182	$1.0000+\mathrm{i}1.2668$	2.6138
5	0.3923	-0.4491	$-1.9306-\mathrm{i}1.0663$	4.4057
6	0.3626	-0.1881	$0.1621+\mathrm{i}0.5940$	3.3108
7	0.2126	-0.1281	$2.1621-\mathrm{i}0.1940$	1.3108
8	0.1026	-1.0881	$-2.2621-\mathrm{i}2.6040$	0.3108
9	0.4026	-0.1481	$-0.7621+\mathrm{i}1.2940$	0.8108

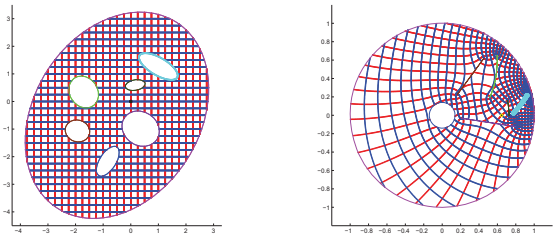

Figure 4 Mapping a region of connectivity seven onto an annulus with spiral slits.

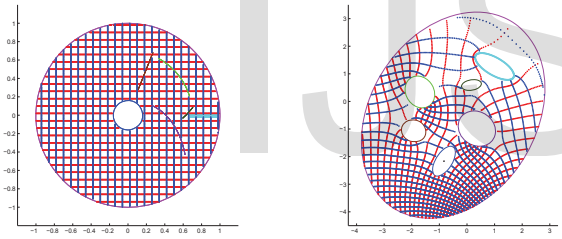

Figure 5 Inverse image of the annulus with spiral slits.

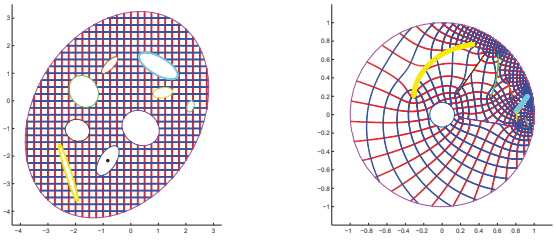

Figure 6 Mapping a region of connectivity ten onto an annulus with spiral slits.

Example 5.3 *Consider a region* Ω *bounded by four rectangles,*

$$\Gamma_0(t)=\begin{cases} t-4-3\mathrm{i}, & 0\le t\le \dfrac{\pi}{2},\\ 4-\left(11-\dfrac{16t}{\pi}\right)\mathrm{i}, & \dfrac{\pi}{2}\le t\le \pi,\\ \dfrac{-16t}{\pi}+20+5\mathrm{i}, & \pi\le t\le \dfrac{3\pi}{2},\\ -4+\left(29-\dfrac{16t}{\pi}\right)\mathrm{i}, & \dfrac{3\pi}{2}\le t\le 2\pi, \end{cases}$$

$$\Gamma_s(t)=\begin{cases} 1-\dfrac{4t}{\pi}-\mathrm{i}, & 0\le t\le \dfrac{\pi}{2},\\ -1+\left(\dfrac{4t}{\pi}-3\right)\mathrm{i}, & \dfrac{\pi}{2}\le t\le \pi,\\ \dfrac{4t}{\pi}-5+\mathrm{i}, & \pi\le t\le \dfrac{3\pi}{2},\\ 1+\left(7-\dfrac{4t}{\pi}\right)\mathrm{i}, & \dfrac{3\pi}{2}\le t\le 2\pi, \end{cases}$$

$$\Gamma_1(t)=-1.5+\mathrm{i}+\Gamma_s,$$
$$\Gamma_2(t)=1.5-1.2\mathrm{i}+\Gamma_s,$$
$$\Gamma_3(t)=1.5+2\mathrm{i}+\Gamma_s,$$

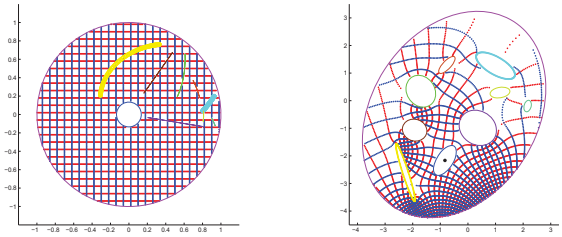

Figure 7 Inverse image of the annulus with spiral slits.

Table 3 Radii comparison for Example 5.2 with [6]

n	32	64	128
$\|c-cN\|_\infty$	1.0(−06)	1.7(−12)	4.4(−16)
$\|R_1-RN_1\|_\infty$	1.2(−07)	2.3(−13)	5.2(−16)
$\|R_2-RN_2\|_\infty$	2.5(−06)	4.5(−12)	1.1(−16)
$\|R_3-RN_3\|_\infty$	2.9(−07)	6.7(−13)	2.4(−16)
$\|R_4-RN_4\|_\infty$	1.3(−06)	2.3(−12)	2.7(−16)
$\|R_5-RN_5\|_\infty$	2.3(−06)	3.8(−12)	1.3(−15)
$\|R_6-RN_6\|_\infty$	1.7(−06)	2.4(−12)	1.6(−16)

Table 4 The numerical values of c, R_i, $i=1,\ldots,9$ for Example 5.2.

n	32	64	128
c	0.6468127386	0.6467702190	0.6467709323
R_1	1.0000000000	1.0000000000	1.0000000000
R_2	0.6586525858	0.6584912008	0.6584906527
R_3	−0.1624735970	−0.1622552127	−0.1622552041
R_4	0.1879050402	0.1877504175	0.1877503706
R_5	0.9591057560	0.9577764470	0.9577732112
R_6	0.2081809532	0.2086356775	0.2086342427
R_7	0.1107244198	0.1129461207	0.1129518147
R_8	0.4205292167	0.4196782143	0.4196760538
R_9	−0.2372178130	−0.2372480822	−0.2372476284

We choose the value of θ_j, $j = 0,1,2,3$ *to be* $\theta = (\pi/2, \pi/3, 0, \pi/2)$, *and* $z_1 = 1.5 + 2\mathrm{i}$. *Mapping function from the original region onto the annulus with spiral slits region and the inverse mapping functions from the annulus with spiral slits region onto the original region. The numerical results are presented in Figures 8–9.*

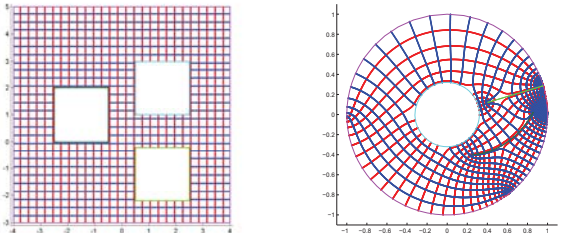

Figure 8 Mapping a region with non-smooth boundaries onto the annulus with spiral slits for Example 5.3.

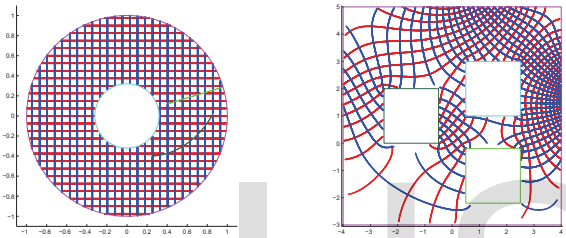

Figure 9 Inverse image of the annulus with spiral slits for Example 5.3.

6 Conclusions

In this paper, we have constructed new boundary integral equations for conformal mapping of multiply connected regions onto an annulus with spiral slits region. We have also constructed a new method to find the values of modulus of $f(z)$. The advantage of our method is that our boundary integral equations are all linear and can be used for the region with smooth and non-smooth boundaries. Several mappings of the test regions of connectivity three, seven and ten with smooth boundaries and connectivity four with non-smooth boundaries were computed numerically using the proposed method. After the boundary values of the mapping function are computed, the interior mapping function are calculated by the means of Cauchy integral formula. And the inverse mapping function from annulus with spiral slits region onto the original regions are computed. The numerical examples presented have illustrated that our boundary integral equation method has high accuracy.

Acknowledgments

This work was supported in part by the Ministry of Higher Education through Department of Mathematics School of Science, University of Sulaimani. And the Malaysian Ministry of Higher Education (MOHE) through the Research Management Centre (RMC), Universiti Teknologi Malaysia. Those supports are gratefully acknowledged.

References

[1] Guo Chun Wen, *Conformal mappings and boundary value problems*, AMS Bookstore, 1992.

[2] Z. Nehari, *Conformal Mapping*, Dover Publication, New York, 1952.

[3] Paul Koebe, "Abhandlungen zur theorie der konformen abbildung", *Acta Mathematica*, vol. 41, no. 1, pp. 305–344, 1916.

[4] Mohamed MS Nasser, "A boundary integral equation for conformal mapping of bounded multiply connected regions", *Computational Methods and Function Theory*, vol. 9, no. 1, pp. 127–143, 2009.

[5] Mohamed MS Nasser, "Numerical conformal mapping via a boundary integral equation with the generalized neumann kernel", *SIAM Journal on Scientific Computing*, vol. 31, no. 3, pp. 1695–1715, 2009.

[6] Mohamed Nasser, "Numerical conformal mapping of multiply connected regions onto the second, third and fourth categories of koebe?s canonical slit domains", *Journal of Mathematical Analysis and Applications*, vol. 382, no. 1, pp. 47–56, 2011.

[7] Rudolf Wegmann and Mohamed Nasser, "The riemann–hilbert problem and the generalized neumann kernel on multiply connected regions", *Journal of Computational and Applied Mathematics*, vol. 214, no. 1, pp. 36–57, 2008.

[8] Ali WK Sangawi, Mohamed Murid, Ali Hassan, and MMS Nasser, "Annulus with circular slit map of bounded multiply connected regions via integral equation method", *Bulletin of the Malaysian Mathematical Sciences Society*, vol. 35, no. 4, pp. 945–959, 2012.

[9] Ali WK Sangawi, Ali HM Murid, and Mohamed MS Nasser, "Linear integral equations for conformal mapping of bounded multiply connected regions onto a disk with circular slits", *Applied Mathematics and Computation*, vol. 218, no. 5, pp. 2055–2068, 2011.

[10] Ali WK Sangawi, Ali HM Murid, and MMS Nasser, "Circular slits map of bounded multiply connected regions", in *Abstract and Applied Analysis*. Hindawi Publishing Corporation, 2012, vol. 2012.

[11] Ali WK Sangawi, Ali HM Murid, and MMS Nasser, "Parallel slits map of bounded multiply connected regions", *Journal of Mathematical Analysis and Applications*, vol. 389, no. 2, pp. 1280–1290, 2012.

[12] Ali WK Sangawi, Ali HM Murid, and Mohamed MS Nasser, "Radial slit maps of bounded multiply connected regions", *Journal of Scientific Computing*, pp. 1–18, 2013.

[13] Ali HM Murid and Laey-Nee Hu, "Numerical experiment on conformal mapping of doubly connected regions onto a disk with a slit", *International Journal of Pure and Applied Mathematics*, vol. 51, no. 4, pp. 589–608, 2009.

[14] Ali HM Murid and Laey-Nee Hu, "Numerical conformal mapping of bounded multiply connected regions by an integral equation method", *Int. J. Contemp. Math. Sciences*, vol. 4, no. 23, pp. 1121–1147, 2009.

[15] Mohamed MS Nasser, Ali HM Murid, M Ismail, and EMA Alejaily, "Boundary integral equations with the generalized neumann kernel for laplaceŠs equation in multiply connected regions", *Applied Mathematics and Computation*, vol. 217, no. 9, pp. 4710–4727, 2011.

[16] Edward B Saff and Arthur David Snider, "Fundamentals of complex analysis with applications to engineering, science, and mathematics", *Prentice Hall, NJ*, 2003.

[17] Johan Helsing and Rikard Ojala, "On the evaluation of layer potentials close to their sources", *Journal of Computational Physics*, vol. 227, no. 5, pp. 2899–2921, 2008.

[18] Kendall E Atkinson, *The numerical solution of integral equations of the second kind*, Number 4. Cambridge university press, 1997.

[19] Philip J Davis and Philip Rabinowitz, *Methods of numerical integration*, Academic Press, Orlando, 1984.

[20] Kendall E Atkinson and KE Atkinson, *A survey of numerical methods for the solution of Fredholm integral equations of the second kind*, vol. 16, Society for Industrial and Applied Mathematics Philadelphia, 1976.